

Fast Inverse Tone Mapping Based on Reinhard's Global Operator with Estimated Parameters

Yuma KINOSHITA[†], Student Member, Sayaka SHIOTA[†], Member, and Hitoshi KIYA^{†a)}, Fellow

SUMMARY This paper proposes a new inverse tone mapping operator (TMO) with estimated parameters. The proposed inverse TMO is based on Reinhard's global operator which is a well-known TMO. Inverse TM operations have two applications: generating an HDR image from an existing LDR one, and reconstructing an original HDR image from the mapped LDR image. The proposed one can be applied to both applications. In the latter application, two parameters used in Reinhard's TMO, i.e. the key value α regarding brightness of a mapped LDR one and the geometric mean \bar{L}_w of an original HDR one, are generally required for carrying out the Reinhard based inverse TMO. In this paper, we show that it is possible to estimate \bar{L}_w from α under some conditions, while α can be also estimated from \bar{L}_w , so that a new inverse TMO with estimated parameter is proposed. Experimental results show that the proposed method outperforms conventional ones for both applications, in terms of high structural similarities and low computational costs.

key words: *HDR image, tone mapping, inverse tone mapping*

1. Introduction

The interest of high dynamic range (HDR) imaging has recently been increasing in various area: photography, medical imaging, computer graphics, on vehicle cameras, aeronautics. Various research works on HDR imaging have so far been reported. Many of these have focused on tone mapping (TM) operations [1]–[7]. TM operations which generate LDR images from HDR ones is required to display HDR ones on conventional LDR devices. Meanwhile, with the availability of high quality display devices, the acquisitions of HDR images or videos become more and more important.

The most common approach to produce HDR images with a LDR detector is to sequentially capture multiple images of the same scene using different exposures [8], [9]. However, this kind of approaches is only suitable for static scenes. Recently, novel HDR-video cameras have been also provided by manufacturers such as the Spheron HDRv and Red HDRx technologies, to produce impressive videos [10], [11]. However, such techniques have a problem, that is the high cost of the overall system. In addition, these approaches are not suitable for reproducing real-world appearance images through legacy LDR images or videos.

Because of such a situation, this paper focuses on inverse TM operators (TMOs) that work on reproducing real-world appearance images through LDR images. Inverse TM

operations have two applications: generating an HDR image from an existing LDR one, and reconstructing an original HDR image from the mapped LDR one. A lot of inverse TMOs for the former application have been proposed [12]–[16]. Huo et al. succeeded in expanding the local dynamic range in dark and bright area by using the dodging and burning algorithm with a S curve operator [15]. Wang et al. proposed an inverse TM operation which conflates pseudo-multiple-exposures HDR images generated from a single LDR image [16]. A high-performance inverse TM operation at low computational cost is generally required because HDR imaging techniques are expected to applied to not only images but also videos. However, the existing inverse TM operations require complex processing for generating high quality HDR images, and moreover, most of them do not support the latter application.

The latter application is used to compression coding an HDR image such as for the JPEG-XT standard [17] and remapping operations [18]. In [18], the Reinhard based inverse TMO without parameters has been proposed. The inverse TMO is designed for an remapping operation that enables to remap an LDR image to another LDR one. However, the inverse TMO is not able to be applied to the former application. In addition, it cannot provide high quality HDR ones for the latter application.

To overcome these problems, we propose a novel inverse TMO which allows us to apply to both applications at low computational cost. The proposed inverse TMO is based on an inverse transform of Reinhard's global operator [19], [20]. Conventionally, two parameters used in Reinhard's TMO, i.e. the key value α regarding brightness of a mapped LDR one and the geometric mean \bar{L}_w of an original HDR one, are generally required for carrying out the Reinhard based inverse TMO [21]. In this paper, we show that the parameter \bar{L}_w can be estimated from α under some conditions, while α can be estimated from \bar{L}_w , so that a new inverse TMO with estimated parameter is proposed.

We evaluate the effectiveness of the proposed inverse TMO in terms of the quality of generated HDR images and the executing time by a number of simulations. Simulation results show that the proposed method is able to outperform conventional ones for both applications, maintaining the structural similarity with a low computational cost.

2. Preparation

A TM operation generates an LDR image I_L from an HDR

Manuscript received February 2, 2017.

Manuscript revised June 6, 2017.

[†]The authors are with Department of Information and Communication Systems, Tokyo Metropolitan University, Tokyo, 191-0065 Japan.

a) E-mail: kiya@tmu.ac.jp

DOI: 10.1587/transfun.E100.A.2248

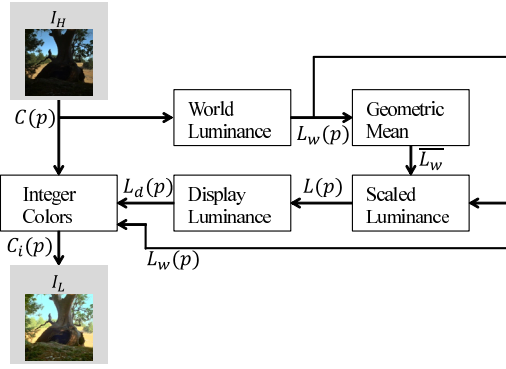


Fig. 1 Photographic tone reproduction.

image I_H . A typical TM operation is reviewed.

2.1 Photographic Tone Reproduction

“Photographic Tone Reproduction” [19] which is a typical TM operation is summarized, here. This TM operation consists of the following six steps (see Fig. 1).

- (a) The world luminance $L_w(p)$ of an HDR image I_H is calculated from RGB pixel values of the HDR image as,

$$L_w(p) = 0.27R(p) + 0.67G(p) + 0.06B(p) \quad (1)$$

where $R(p)$, $G(p)$ and $B(p)$ are RGB pixel values of the HDR image with a pixel p , respectively.

- (b) The geometric mean \bar{L}_w of the world luminance $L_w(p)$ is calculated as follows:

$$\bar{L}_w = \exp\left(\frac{1}{N} \sum_{p=1}^N \log L_w(p)\right) \quad (2)$$

where N is the total number of pixels in the input HDR image I_H . If Eq. (2) has singularities at some pixels i.e. $L_w(p) = 0$, \bar{L}_w is calculated as follows:

$$\bar{L}_w = \exp\left(\frac{1}{N} \left(\sum_{p \notin B} \log L_w(p) + \sum_{p \in B} \log \epsilon \right) \right) \quad (3)$$

where $B = \{p | L_w(p) = 0\}$ and ϵ is a small value.

- (c) The scaled luminance $L(p)$ is calculated as

$$L(p) = \frac{\alpha}{\bar{L}_w} L_w(p) \quad (4)$$

where $\alpha \in [0, 1]$ is the parameter called “key value”, which indicates subjectively if the scene is light, normal, or dark [19].

- (d) The display luminance $L_d(p)$ is calculated by using a TMO $y(\cdot)$ as follows:

$$L_d(p) = y(L(p)). \quad (5)$$

The Reinhard's global operator [19] which is a well-known TMO is given by

$$L_d(p) = \frac{L(p)}{1 + L(p)}. \quad (6)$$

- (e) The floating-point pixel values $C_f(p)$ of the LDR image is calculated as follows:

$$C_f(p) = \frac{L_d(p)}{L_w(p)} C(p) \quad (7)$$

where $C(p) \in \{R(p), G(p), B(p)\}$ is the floating-point RGB value of the input HDR image I_H , and $C_f(p) \in \{R_f(p), G_f(p), B_f(p)\}$. Besides, the gamma correction is performed for $C_f(p)$ as needed.

- (f) The 8-bit color RGB values $C_i(p)$ of the LDR image I_L is derived from

$$C_i(p) = \text{round}(C_f(p) \cdot 255) \quad (8)$$

where $\text{round}(x)$ rounds x to its nearest integer value, and $C_i(p) \in \{R_i(p), G_i(p), B_i(p)\}$.

2.2 Scenarios

This paper proposes a novel inverse TMO to estimate HDR images from LDR ones. The proposed method has two scenarios from the difference of applications.

Scenario 1: Inverse TM of LDR images mapped by Reinhard's global operator

The first scenario is to reconstruct the original HDR image from an LDR image mapped by Reinhard's global operator. The inverse function of the Reinhard's global operator is given as, from Eqs. (4) and (6)

$$L_w(p) = \frac{\bar{L}_w}{\alpha} \cdot L(p) = \frac{\bar{L}_w \cdot L_d(p)}{\alpha(1 - L_d(p))}. \quad (9)$$

To calculate this equation, the original HDR image I_H or two parameters (α and \bar{L}_w) are required to be stored. In particular, every image has a different \bar{L}_w value. Therefore, when we map a number of HDR images or videos to LDR ones, all \bar{L}_w values have to be stored to carry out Eq. (9). On the other hand, α is commonly used for multiple images.

In this paper, a new inverse TMO with one parameter is proposed, where the other parameter is estimated.

Scenario 2: Inverse TM of existing LDR images

The second scenario is to create HDR images from existing LDR ones captured in legacy LDR format. In this case, there is no information on the relationship between the LDR ones and the real scenes. Therefore, it is difficult to determine operators or parameters for inverse TM. As a result, conventional inverse TM operations require high computing cost processing for generating high quality HDR images from existing LDR ones.

By using the proposed method, fast inverse TM is able

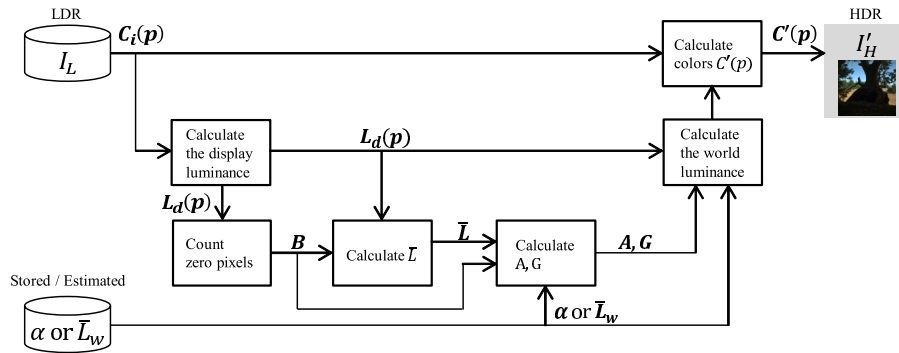


Fig. 2 Proposed inverse tone mapping operation.

to be carried out without any parameters even when LDR images are not generated by Reinhard's global operator. In other words, two parameters, i.e. α and \bar{L}_w are estimated for Scenario 2. Therefore the proposed method is effective for both applications, while keeping a high structural similarity and a low computational cost.

3. Proposed Inverse TM Operation

Assuming the use of the Reinhard's global operator, a new inverse TM operation based on photographic tone reproduction is proposed.

3.1 Inverse TMO Based on the Reinhard's TMO

The proposed inverse TMO is shown as

$$L'_w(p) = \frac{G}{A} \cdot L(p) = \frac{G \cdot L_d(p)}{A(1 - L_d(p))}. \quad (10)$$

As described later, the parameters A and G are given by using α or \bar{L}_w .

(i) Given α , A and G are calculated as

$$\begin{cases} A = \alpha \\ G = \exp\left(\frac{N}{|B|} \log \bar{L} - \frac{|B^C|}{|B|} \log \alpha\right). \end{cases} \quad (11)$$

B^C is a complement of the set B i.e. $B^C = \{p | L_w(p) \neq 0\}$ and the geometric mean of the scaled luminance $L(p)$, \bar{L} is given by, as well as in Eq. (3)

$$\begin{aligned} \bar{L} &= \exp\left(\frac{1}{N} \left(\sum_{p \notin B} \log L(p) + \sum_{p \in B} \log \epsilon \right)\right) \\ &= \exp\left(\frac{1}{N} \left(\sum_{p \notin B} \log \frac{L_d(p)}{1 - L_d(p)} + \sum_{p \in B} \log \epsilon \right)\right). \end{aligned} \quad (12)$$

Compared Eq. (10) with Eq. (9), parameters α and \bar{L}_w are replaced with A and G in Eq. (9).

Note that $|B| \neq 0$ is assumed in Eq. (11). Therefore, to calculate Eq. (11), the minimum value in the world luminance $L_w(p)$ is replaced with zero value, if image

I_H satisfies $|B| = 0$.

(ii) Given \bar{L}_w , A and G are calculated as

$$\begin{cases} A = \exp\left(\frac{N}{|B^C|} \log \bar{L} - \frac{|B|}{|B^C|} \log \bar{L}_w\right) \\ G = \bar{L}_w. \end{cases} \quad (13)$$

In this case, Eq. (13) is calculable even when $|B| = 0$.

3.2 Proposed Procedure

The procedure for generating an HDR image I'_H from an LDR image I_L is summarized as follows (see Fig. 2).

Scenario 1

The proposed inverse TMO consists of six steps as follows.

1. Calculate a display luminance $L_d(p)$ from RGB values of an LDR image as

$$L_d(p) = \frac{0.27R_i(p) + 0.67G_i(p) + 0.06B_i(p)}{255}. \quad (14)$$

2. Let B be a set of pixels p such that $L_d(p) = 0$.
3. Calculate \bar{L} by Eq. (12).
4. Calculate parameters A and G .
 - a. When α is given, calculate parameters A and G according to Eq. (11). Note that $|B| \neq 0$ is assumed as shown in 3.1.
 - b. When \bar{L}_w is given, calculate parameters A and G according to Eq. (13).
5. Calculate a world luminance $L'_w(p)$ according to Eq. (10) using A and G .
6. Obtain an HDR image I'_H with color components $C'(p) \in \{R'(p), G'(p), B'(p)\}$ as follows:

$$C'(p) = \frac{L'_w(p)}{L_d(p)} \cdot C_f(p) = \frac{L'_w(p)}{L_d(p)} \cdot \frac{C_i(p)}{255}. \quad (15)$$

Scenario 2

The procedure for creating an HDR image from an existing LDR one is summarized, here. We cannot generally know α and \bar{L}_w for Scenario 2. The difference between two scenarios is only the selection of the parameter $A = \alpha$ at step

4.a. in the above procedure, because G can be estimated by using α as indicated in Eq. (11).

In this paper, α is given by

$$\alpha = \bar{L}, \quad (16)$$

where α controls the brightness of the LDR one I_L if an existing LDR image is mapped by Reinhard's global operator. The validity of Eq. (16) will be shown in 3.3. \bar{L} can be calculated from I_L , so that the proposed method is easily carried out.

3.3 Deriving the Proposed Inverse TMO

The calculating formulas of parameters A and G shown in Eq. (10) is derived here.

First, we consider the geometric mean \bar{L} of the scaled luminance $L(p)$. The geometric mean \bar{L} is calculated by substituting Eq. (4) into Eq. (12),

$$\begin{aligned} \bar{L} &= \exp\left(\frac{1}{N}\left(\sum_{p \notin B} \log \frac{\alpha}{\bar{L}_w} L_w(p) + \sum_{p \in B} \log \epsilon\right)\right) \\ &= \exp\left(\frac{1}{N} \sum_{p \notin B} \log \alpha - \frac{1}{N} \sum_{p \notin B} \log \bar{L}_w\right) \\ &\quad \cdot \exp\left(\frac{1}{N} \sum_{p \notin B} \log L_w(p) + \frac{1}{N} \sum_{p \in B} \log \epsilon\right) \\ &= \exp\left(\frac{|B^C|}{N} \log \alpha + \frac{|B|}{N} \log \bar{L}_w\right). \end{aligned} \quad (17)$$

From Eq. (17), we achieve relational expressions, which correspond to Eqs. (11) and (13) respectively, as follows:

$$\alpha = \exp\left(\frac{N}{|B^C|} \log \bar{L} - \frac{|B|}{|B^C|} \log \bar{L}_w\right) \quad (18)$$

$$\bar{L}_w = \exp\left(\frac{N}{|B|} \log \bar{L} - \frac{|B^C|}{|B|} \log \alpha\right). \quad (19)$$

Therefore, replacing α and \bar{L}_w with A and G respectively, we arrive at Eqs. (11) and (13). As a result, the parameter α is calculated by Eq. (18), while \bar{L}_w is also done by Eq. (19), under the condition that α or \bar{L}_w is known, since \bar{L} is calculated from the mapped LDR image.

In addition, when $N \approx |B^C|$, we obtain the relationship between α and \bar{L} from Eq. (18) as

$$\alpha \approx \bar{L}. \quad (20)$$

This conclusion enables to perform the proposed inverse TMO for Scenario 2, even though the parameters α and \bar{L}_w are unknown.

4. Simulation

We evaluated the proposed inverse TMO in terms of the quality of a generated HDR image I'_H and the executing time

Table 1 Machine spec used in the simulation.

Processor	Intel Core i7-3770 3.40 GHz
Memory	16 GB
OS	ubuntu 14.04 LTS
Software	MATLAB R2014b

by a number of simulations with HDR images.

4.1 Evaluating the Proposed Method

To evaluate the quality of HDR images generated by the proposed inverse TMO, objective quality assessments and reference HDR images are needed. HDR images generally have a much wider dynamic range than that of LDR ones. For this reason, conventional quality assessments such as PSNR or SSIM are not suited to evaluate the quality of HDR images. Therefore, various research works on evaluating HDR images have so far been done [22]. In this paper, we will use HDR-VDP-2.2 [23] and PU encoding [24] + MS-SSIM [25] as typical quality metrics to evaluate the quality of HDR images.

4.2 Simulation Conditions

We used 60 HDR images selected from the databases [26], [27] for the evaluation (see Fig. 3). The proposed method was compared with five inverse TMOs, i.e. the conventional inverse operation using Eq. (9) with the true parameters, the conventional one using Eq. (9) without parameters [18], PMET [16], Kuo's method [14] and Huo's method [15]. The proposed method and the conventional ones in Eq. (9) are called inverse photographic tone reproduction (IPTR) in the following section. The simulation was run on a PC, with a 3.4 GHz processor and a main memory of 16 Gbytes (see Table 1).

Scenario 1

The following procedure was carried out to evaluate the effectiveness.

1. Map an HDR image I_H to an LDR image I_L by Reinhard's global operator.
2. Carry out an inverse TMO for I_L to obtain I'_H .
3. Evaluate the similarity between images I'_H and I_H , in accordance with the criterions i.e. HDR-VDP-2.2 MOS value [23] and PU encoding [24]+ MS-SSIM [25].

Scenario 2

For Scenario 2, there are generally no HDR images, but they are needed to evaluate the quality of images generated inverse TMOs. Thus, LDR images I_L used for the simulation were generated from HDR ones by ten TMOs selected from the literature [28], respectively. The ten TMOs are: 1. Reinhard's global TMO, 2. Reinhard's global TMO using a parameter L_{white} , 3. Reinhard's local TMO, 4. Logarithmic TMO, 5. Tumblin's TMO, 6. Schlick's TMO, 7. Chiu's TMO, 8. Ashikhmin's TMO, 9. Fattal's TMO, and 10. Gamma TMO. Other conditions were the same as in the procedure for Scenario 1.



Fig. 3 Examples of tone mapped images.

Table 2 Experimental results for Scenario 1 (HDR-VDP-2.2).

inverse TMO	IPTR (proposed, with α)	IPTR (proposed, with \bar{L}_w)	IPTR (with two parameters)	IPTR [18] (without parameters)	PMET [16]	Kuo's ITMO [14]	Huo's ITMO [15]
Adjuster	58.25	58.32	58.17	57.81	57.41	42.65	53.13
Cannon	95.00	95.53	95.53	70.69	55.17	49.92	56.58
Desk	49.45	49.76	49.76	50.50	44.66	43.88	43.89
Flowers	83.22	83.22	83.22	63.92	54.70	58.20	55.39
Impact	39.47	39.45	39.45	35.34	41.01	27.22	41.94
Kapaa	90.55	90.88	90.88	64.21	54.47	44.54	55.46
Memorial	49.60	49.71	49.61	51.61	45.33	39.60	44.65
Mirror Pattern	47.71	47.74	47.74	37.27	47.88	44.29	48.24
Rend01	80.39	80.39	80.39	56.98	72.03	42.37	77.34
Tree	54.21	55.18	55.18	55.65	51.92	34.31	51.57

Table 3 Experimental results for Scenario 1 (PU encoding + MS-SSIM).

inverse TMO	IPTR (proposed, with α)	IPTR (proposed, with \bar{L}_w)	IPTR (with two parameters)	IPTR [18] (without parameters)	PMET [16]	Kuo's ITMO [14]	Huo's ITMO [15]
Adjuster	0.991	0.991	0.991	0.931	0.944	0.534	0.909
Cannon	1.000	1.000	1.000	0.990	0.773	0.744	0.747
Desk	0.933	0.938	0.938	0.940	0.783	0.661	0.738
Flowers	1.000	1.000	1.000	0.947	0.706	0.871	0.675
Impact	0.845	0.855	0.855	0.496	0.727	0.091	0.749
Kapaa	1.000	1.000	1.000	0.950	0.702	0.524	0.670
Memorial	0.981	0.982	0.981	0.961	0.879	0.581	0.856
Mirror Pattern	0.674	0.677	0.677	0.679	0.794	0.666	0.670
Rend01	1.000	1.000	1.000	0.803	0.989	0.487	0.999
Tree	0.973	0.978	0.978	0.944	0.892	0.295	0.868

4.3 Simulation Results

Figure 4 illustrates the average executing time when each

inverse TMO is carried out 100 times for 60 images. From the figure, the proposed inverse TMO has much lower computational cost than the others while the proposed one takes a little more time than IPTR with two parameters. On the

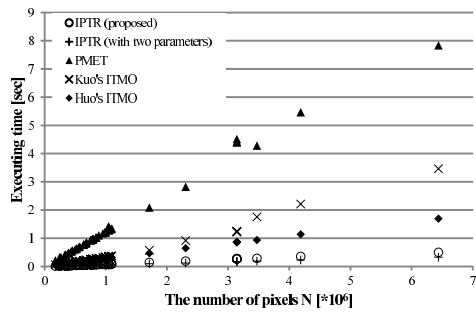


Fig. 4 Executing time of inverse TMOs.

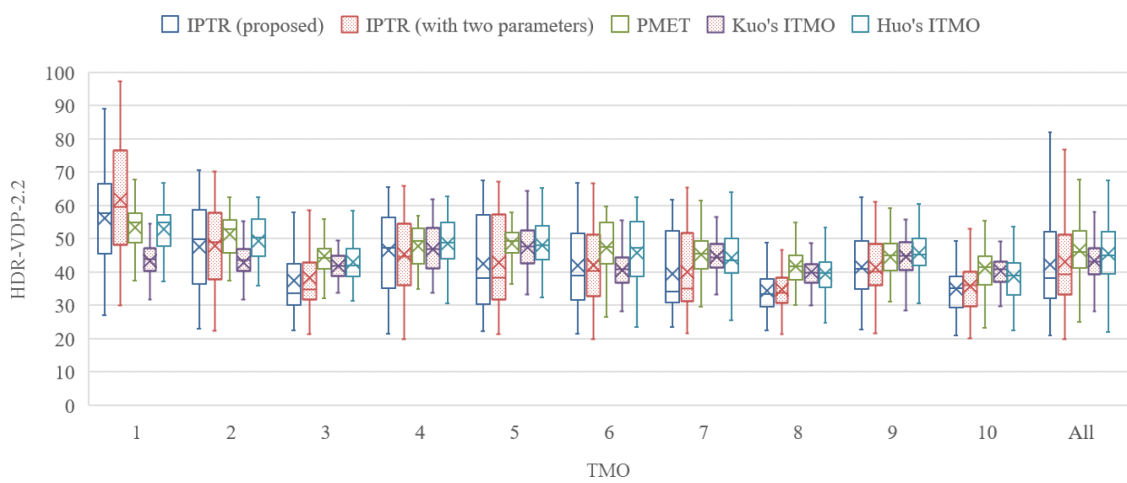


Fig. 5 Experimental results for Scenario 2 (HDR-VDP-2.2). The band inside the box and the cross indicate the median and the average value, respectively. The TMOs are: 1. Reinhard's global TMO, 2. Reinhard's global TMO using a parameter L_{white} , 3. Reinhard's local TMO, 4. Logarithmic TMO, 5. Tumblin's TMO, 6. Schlick's TMO, 7. Chiu's TMO, 8. Ashikhmin's TMO, 9. Fattal's TMO, and 10. Gamma TMO.

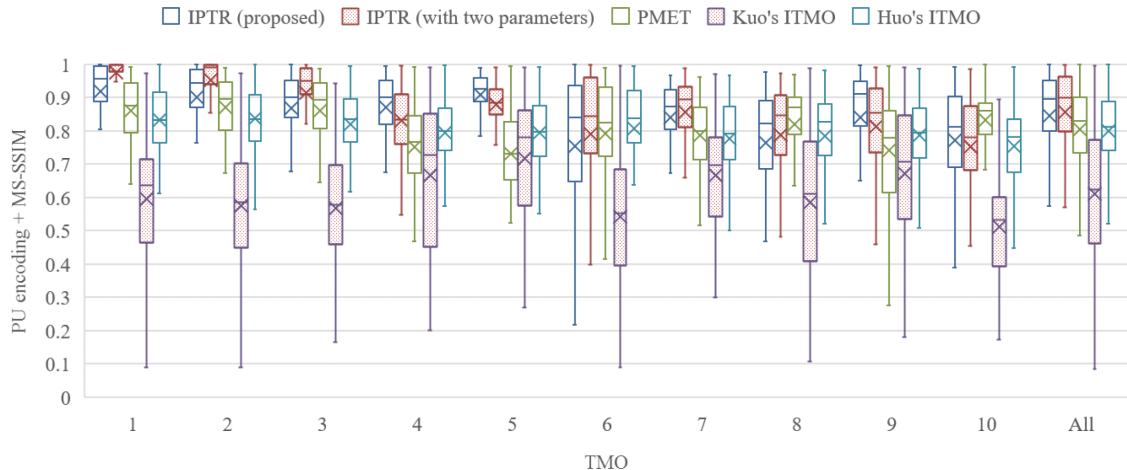


Fig. 6 Experimental results for Scenario 2 (PU encoding + MS-SSIM). The band inside the box and the cross indicate the median and the average value, respectively. The TMOs are: 1. Reinhard's global TMO, 2. Reinhard's global TMO using a parameter L_{white} , 3. Reinhard's local TMO, 4. Logarithmic TMO, 5. Tumblin's TMO, 6. Schlick's TMO, 7. Chiu's TMO, 8. Ashikhmin's TMO, 9. Fattal's TMO, and 10. Gamma TMO.

other hand, PMET has the largest computational cost.

Tables 2 and 3 denote the scores of similarities between HDR images I'_H and I_H which were evaluated by HDR-VDP-2.2 $\in [0, 100]$ and PU encoding + MS-SSIM $\in [0, 1]$, whose larger score indicates a higher similarity between two images.

Figures 5 and 6 also illustrate the scores of similarities between HDR images I'_H and I_H as box plots. The box plots are drawn to visualize the distribution of the scores: the boxes span from 25th to 75th percentile, referred to as P_{25} and P_{75} , and the whiskers show the maximum and minimum values in the range of $[P_{25} - 1.5(P_{75} - P_{25}), P_{75} + 1.5(P_{75} - P_{25})]$. In addition, the band inside the box is the median and the cross is the average value.

Scenario 1

Tables 2 and 3 show that the proposed method can reconstruct HDR images with high quality, and the quality is almost the same as that of IPTR with two parameters. A slightly difference between them are caused due to quantization error at Eq.(8). In addition, the effectiveness of calculating parameters A and G is confirmed since the proposed method outperforms IPTR without parameters. These results denote that the proposed inverse TMO is effective to reconstruct original HDR images from mapped LDR ones.

Scenario 2

Experimental results are illustrated in Figs. 5 and 6. Figure 5 shows that the proposed method can reconstruct an HDR image from an LDR one, mapped by Reinhard's global operator, with very high quality (see "TMO 1" in Fig. 5). On the other hand, in the cases of other TMOs, the proposed method do not have higher quality for other TMOs than conventional ones. As a result, the total results of each inverse TMO for all TMOs are almost the same as shown in "All" in Fig. 5. Figure 6 illustrates that the proposed inverse TMO provides better MS-SSIM scores in terms of both median values and average ones than PMET, Kuo's ITMO and Huo's ITMO, but PMET has the best HDR-VDP-2.2 score as shown in Fig. 5. From Fig. 6, HDR images reconstructed by the proposed method has a high structural similarity, compared with other inverse TMOs, because MS-SSIM measures the structural similarity between two images [22].

On the other hand, HDR-VDP-2.2 indicates the visible differences between two images, but it does not take into account the structural similarity.

From these results, it is shown that the proposed inverse TMO allows us to reconstruct an HDR image from an LDR one, mapped by Reinhard's global operator, with a low visible difference and a high structural similarity. Even if an LDR one is not mapped by Reinhard's global operator, the proposed method can produce an HDR image with high quality regarding the structural similarity. Therefore, it is confirmed that the proposed method is useful for two scenarios, and the resulting HDR images have a high structural similarity. In addition, it is carried out at a low computational cost.

5. Conclusion

This paper has proposed a novel inverse TMO with estimated parameters, which is based on Reinhard's global operator. The proposed inverse TMO can be applied to two applications: reconstructing an original HDR image from the mapped LDR image, and generating an HDR image from an existing LDR one. We also showed that it is possible to calculate \bar{L}_w from α under some conditions, while α can be estimated from \bar{L}_w . The simulation results showed that the proposed method outperforms conventional ones for both applications at a low computational cost. In particular, HDR images generated by the proposed method have a high

structural similarity.

References

- [1] J.W. Lee, R.H. Park, and S. Chang, "Local tone mapping using the k-means algorithm and automatic gamma setting," *IEEE Trans. Consum. Electron.*, vol.57, no.1, pp.209–217, 2011.
- [2] Z. Zhu, Z. Li, S. Wu, and P. Fränti, "Noise reduced high dynamic range tone mapping using information content weights," *Acoustics, Speech and Signal Processing (ICASSP)*, 2015 IEEE International Conference on, pp.1255–1259, 2015.
- [3] J. Shen, S. Fang, H. Zhao, X. Jin, and H. Sun, "Fast approximation of trilateral filter for tone mapping using a signal processing approach," *Signal Process.*, vol.89, no.5, pp.901–907, 2009.
- [4] S. Thakur, M. Sivasubramanian, K. Nallaperumal, K. Marappan, and N. Vishwanath, "Fast tone mapping for high dynamic range images," *Computational Intelligence and Computing Research (ICCIC)*, 2013 IEEE International Conference on, pp.1–4, IEEE, 2013.
- [5] T. Dobashi, A. Tashiro, M. Iwashashi, and H. Kiya, "A fixed-point implementation of tone mapping operation for hdr images expressed in floating-point format," *APSIPA Trans. Signal and Information Processing*, vol.3, no.e11, pp.1–11, 2014.
- [6] T. Murofushi, M. Iwashashi, and H. Kiya, "An integer tone mapping operation for hdr images expressed in floating point data," 2013 IEEE International Conference on Acoustics, Speech and Signal Processing (ICASSP), pp.2479–2483, 2013.
- [7] M. Iwashashi and H. Kiya, "Two layer lossless coding of hdr images," 2013 IEEE International Conference on Acoustics, Speech and Signal Processing (ICASSP), pp.1340–1344, 2013.
- [8] P.E. Debevec and J. Malik, "Recovering high dynamic range radiance maps from photographs," *ACM SIGGRAPH 2008 classes*, p.31, ACM, 2008.
- [9] S.K. Nayar and T. Mitsunaga, "High dynamic range imaging: Spatially varying pixel exposures," *Computer Vision and Pattern Recognition, 2000. Proceedings. IEEE Conference on*, pp.472–479, IEEE, 2000.
- [10] M. Schöberl, J. Keinert, M. Ziegler, J. Seiler, M. Niehaus, G. Schuller, A. Kaup, and S. Foessel, "Evaluation of a high dynamic range video camera with non-regular sensor," *IS&T/SPIE Electronic Imaging*, pp.86600M–86600M, International Society for Optics and Photonics, 2013.
- [11] A. Chalmers, G. Bonnet, F. Banterle, P. Dubla, K. Debattista, A. Artusi, and C. Moir, "High-dynamic-range video solution," *ACM SIGGRAPH ASIA 2009 Art Gallery & Emerging Technologies: Adaptation*, p.71, ACM, 2009.
- [12] F. Banterle, P. Ledda, K. Debattista, and A. Chalmers, "Inverse tone mapping," *Proc. 4th International Conference on Computer Graphics and Interactive Techniques in Australasia and Southeast Asia*, pp.349–356, ACM, 2006.
- [13] A.G. Rempel, M. Trentacoste, H. Seetzen, H.D. Young, W. Heidrich, L. Whitehead, and G. Ward, "Ldr2hdr: On-the-fly reverse tone mapping of legacy video and photographs," *ACM Transactions on Graphics (TOG)*, vol.26, no.3, p.39, 2007.
- [14] P.H. Kuo, C.S. Tang, and S.Y. Chien, "Content-adaptive inverse tone mapping," *Visual Communications and Image Processing (VCIP)*, pp.1–6, IEEE, 2012.
- [15] H. Youngquing, Y. Fan, and V. Brost, "Dodging and burning inspired inverse tone mapping algorithm," *J. Computational Information Systems*, vol.9, no.9, pp.3461–3468, 2013.
- [16] T.H. Wang, C.W. Chiu, W.C. Wu, J.W. Wang, C.Y. Lin, C.T. Chiu, and J.J. Liou, "Pseudo-multiple-exposure-based tone fusion with local region adjustment," *IEEE Trans. Multimedia*, vol.17, no.4, pp.470–484, 2015.
- [17] ISO/IEC, "ISO/IEC 18477 Information technology - Scalable compression and coding of continuous-tone still images," 2015.
- [18] Y. Kinoshita, S. Shiota, M. Iwashashi, and H. Kiya, "An remapping operation without tone mapping parameters for hdr images," *IEICE*

- Trans. Fundamentals, vol.E99-A, no.11, pp.1955–1961, Nov. 2016.
- [19] E. Reinhard, M. Stark, P. Shirley, and J. Ferwerda, “Photographic tone reproduction for digital images,” ACM Trans. Graph. (TOG), vol.21, no.3, pp.267–276, 2002.
 - [20] E. Reinhard, W. Heidrich, P. Debevec, S. Pattanaik, G. Ward, and K. Myszkowski, High Dynamic Range Imaging: Acquisition, Display, and Image-Based Lighting, Morgan Kaufmann, 2010.
 - [21] Y. Kinoshita, S. Shiota, and H. Kiya, “Fast inverse tone mapping with reinhard's global operator,” 2017 IEEE International Conference on Acoustics, Speech and Signal Processing (ICASSP), pp.1972–1976, IEEE, 2017.
 - [22] P. Hanhart, M.V. Bernardo, M. Pereira, A.M. Pinheiro, and T. Ebrahimi, “Benchmarking of objective quality metrics for hdr image quality assessment,” EURASIP Journal on Image and Video Processing, vol.2015, no.1, pp.1–18, 2015.
 - [23] M. Narwaria, R.K. Mantiuk, M.P. Da Silva, and P. Le Callet, “Hdr-vdp-2.2: A calibrated method for objective quality prediction of high-dynamic range and standard images,” J. Electron. Imaging, vol.24, no.1, p.010501, 2015.
 - [24] T.O. Aydin, R. Mantiuk, and H.P. Seidel, “Extending quality metrics to full luminance range images,” Electronic Imaging 2008, pp.68060B–68060B, International Society for Optics and Photonics, 2008.
 - [25] Z. Wang, E.P. Simoncelli, and A.C. Bovik, “Multiscale structural similarity for image quality assessment,” Signals, Systems and Computers, 2004. Conference Record of the Thirty-Seventh Asilomar Conference on, pp.1398–1402, IEEE, 2003.
 - [26] “Github - openexr.” <https://github.com/openexr/>
 - [27] “High dynamic range image examples.” <http://www.anyhere.com/gward/hdrenc/pages/originals.html>
 - [28] F. Banterle, A. Artusi, K. Debattista, and A. Chalmers, Advanced High Dynamic Range Imaging: Theory and Practice, AK Peters (CRC Press), Natick, MA, USA, 2011.



Hitoshi Kiya received his B.Eng. and M.Eng. degrees from Nagaoka University of Technology, Japan, in 1980 and 1982, respectively, and his D.Eng. degree from Tokyo Metropolitan University in 1987. In 1982, he joined Tokyo Metropolitan University as an Assistant Professor, where he became a Full Professor in 2000. From 1995 to 1996, he attended the University of Sydney, Australia as a Visiting Fellow. He was/is the Chair of IEEE Signal Processing Society Japan Chapter, an Associate

Editor for IEEE Trans. Image Processing, IEEE Trans. Signal Processing and IEEE Trans. Information Forensics and Security, respectively. He also serves/served as the President of IEICE Engineering Sciences Society (ESS), the Editor-in-Chief for IEICE ESS Publications, and the President-Elect of APSIPA. His research interests are in the area of signal and image processing including multirate signal processing, and security for multimedia. He received the IWAIT Best Paper Award in 2014 and 2015, IEEE ISPACS Best Paper Award in 2016, the ITE Niwa-Takayanagi Best Paper Award in 2012, the Telecommunications Advancement Foundation Award in 2011, the IEICE ESS Contribution Award in 2010, and the IEICE Best Paper Award in 2008. He is a Fellow Member of IEEE, IEICE and ITE.



Yuma Kinoshita received his B.Eng. degree from Tokyo Metropolitan University, Japan in 2016. From 2016, he has been a Master course student at Tokyo Metropolitan University. He received IEEE ISPACS Best Paper Award in 2016. His research interests are in the area of image processing. He is a student member of IEEE and IEICE.



Sayaka Shiota received the B.E., M.E. and Ph.D. degrees in intelligence and computer science, Engineering and engineering simulation from Nagoya Institute of Technology, Nagoya, Japan in 2007, 2009 and 2012, respectively. From February 2013 to March 2014, she had worked at the Institute professor. In April of 2014, she joined Tokyo Metropolitan University as an Assistant Professor. Her research interests include statistical speech recognition and speaker verification. She is a member of the

Acoustical Society of Japan (ASJ), the IEICE, and the IEEE.